Journal of Imaging Science and Technology® 53(5): 050503–050503-13, 2009.

New Nonphotorealistic Shading Algorithm to Improve the Perceptual Quality of Two-Dimensional Images

Tatsumi Watanabe▲
Digital & Network Technology Development Center, Panasonic Corporation, 1006 Kadoma, Kadoma City, Osaka 571-8501, Japan
E-mail: watanabe.tatsumi@jp.panasonic.com

Shuichi Ojima
Faculty of Computer and Information Sciences, Sojo University, 4-22-1 Ikeda, Kumamoto City, Kumamoto 860-0082, Japan

Abstract. *We propose a nonphotorealistic shading algorithm to improve the perceptual quality of two-dimensional natural images that do not have depth information. Shading plays an important role in the human perception of three-dimensional shapes; however, an appropriate normal is indispensable to the shading approach. Generally, it is pointed out that luminance variation due to shading is useful as an indicator of shape and that the depth values are strongly related to the luminance distribution of the object. Therefore, first, we compute the surface normals from the variation in the luminance at each pixel. Second, we enhance the shade by controlling the azimuth of the normals on the basis of the angle between each normal and a given light source direction. From experimental results of the natural images and subjective test, we demonstrate that the three-dimensional (3D) appearance can be improved by our shading approach. Moreover, we also propose an advanced shading approach, which is the combination of our shading approach and the process of selecting the suitable light direction, and we show the performance of selecting the suitable light direction and also demonstrate that the 3D appearance can be more enhanced by using the suitable light direction. Last, we investigate the possibilities of the advanced shading approach. © 2009 Society for Imaging Science and Technology.*
[DOI: 10.2352/J.ImagingSci.Technol.2009.53.5.050503]

INTRODUCTION

Due to various limitations of display devices or image sources, most displays cannot transmit the actual physical stimulus from the real world to human eyes. The loss of the three-dimensional (3D) experience is often pointed out as a disadvantage of displays. In high quality image processing, the contrast or sharpness enhancement by considering human eye perception has already been proposed.[1–6] However, the effect on improving the 3D experience in previous approaches has been inadequate, although this improvement was not their main focus points of these approaches.

In contrast, there have been a few approaches that have targeted the enhancement of the 3D experience. For example, in the field of computer graphics (CG), "nonphotorealistic shading approaches" have been proposed, which focus on the artistic techniques rather than the faithful expressions of the image. These approaches usually alter the local textures by controlling shape information such as surface normals.

Saito and Takahashi proposed the effect of local enhancement of images using depth information. They improved the rendering of an object by utilizing the depth buffer and its derivatives for the creation of contours, creases, and hatching strikes.[7]

An artistic contrast enhancement was employed by Winkenbach and Salesin.[8] They partly removed the texture details of surfaces for artistic reasons and for a better perception of synthetic drawings.

Gooch et al. presented a nonphotorealistic lighting approach that provides a better and sharper comprehension by mapping the change in surface orientation into variations in hue instead of brightness variations,[9] and they proposed the lit sphere approach that extracts artistic shading models from actual paintings.[10] Unfortunately, much of the original brush texture is lost as the shading gradient is captured.

Further, Cignoni et al. modified the surface normals in order to alter the shading of objects.[11] Similarly, in this approach the edges are emphasized and the surfaces are shaded slightly to particularly diminish the produced dull appearance. Moreover, Rusinkiewicz et al. proposed a nonphotorealistic shading model, motivated by techniques for cartographic terrain relief, based on the dynamic adjustment of the effective light position of different areas of the surface.[12] Luft proposed a method to locally enhance the contrast based on the difference between the original depth buffer content and a low-pass filtered copy.[13]

However, the common problem of all these approaches is that they assume that the surface normals in the two-dimensional (2D) image are known and that we cannot directly apply these approaches to 2D natural images that include real scenes.

As in other approaches, Pearson and Robinson described lines dependent on view and lighting.[14] They seek thin dark regions in an image lit by a single source in the same horizontal plane as the view vector.

Ni et al.[15] applied the object-space suggestive contour

▲IS&T Member.

Received Sep. 5, 2008; accepted for publication Jun. 6, 2009; published online Aug. 27, 2009.
1062-3701/2009/53(5)/050503/13/$20.00.

algorithm to a multiscale mesh that smoothly adapts its detail to suit the viewing conditions. While effective, the multiscale representation requires preprocessing time to build, plus significantly more memory at run-time than the original mesh. Juddy et al.[16] presented a new object-space definition of lines—"apparent ridges"—that extracts ridges using a view-dependent measure of curvature. The lines are related to the shaded image: they appear where the surface is most likely to reveal high shading contrast under arbitrary lighting.

However, these line approaches also need the extraction of suggestive contour and the suitable contour cannot easily be obtained for the 2D natural images that include real scenes. In contrast, in computer vision, the approaches to recover the surface normals from a gradual variation in the image are called shape from shading (SFS) approaches. In this approach, surface normals are computed under some constraints.[17,18] Therefore, we applied the "shading" concept as in the CG rendering to enhance the 3D experience in the area.[19]

In this article, we propose a new nonphotorealistic shading approach to improve the perception of the 3D shape in 2D natural images. First, we assume the surface normals in the natural scene images by an approach similar to SFS. Second, we enhance the shade by controlling the azimuth of the normals on the basis of the angle between each normal and a given light source direction. Further, to enhance the perception of the 3D shape with more efficiency, we study the process by which the suitable light directions are selected according to the luminance distribution in images, and we also propose the advanced shading approach, which is the combination of our shading approach and this process of selecting the suitable light directions. From the experimental results of natural images and subjective test, we show that the 3D appearance of the output image obtained by our shading approach is better than that of the original 2D image. Moreover, we show the performance of the selection process of the suitable light directions according to the luminance distribution. We also demonstrate that the 3D appearance can be further improved by using the advanced shading approach. In further discussion, we show that the curvature of surface quantitatively increases with surface normal, which is related to a gradual curvature of luminance, from the experimental result of the CG image, and we also discuss the possibilities of advanced shading approaches on the view of effect using multiple light directions.

PROPOSED APPROACH

To achieve a more natural and sufficient effect, we have extended the concept of "nonphotorealistic shading" by detecting surfaces with a gentle curvature and applying the shading concept as in the CG rendering to enhance the 3D experience in the area.

The general procedure for enhancing the 3D effect in 2D images by our approach is as follows:

(a) Detecting surfaces with a gentle curvature and estimating the normals, which express a 3D shape, using the SFS technique in COMPUTER VISION.[17,18]
(b) Transforming the direction of normals to enhance the curvature of the 3D shape in local areas followed by a shading approach using the transformed normals.
(c) Enhancing the range of the modified luminance distribution.

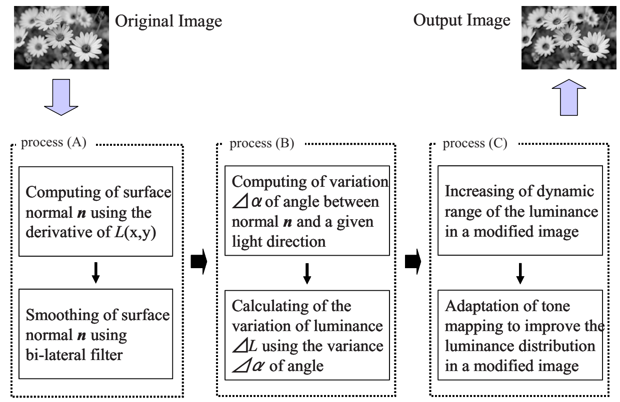

Figure 1. Overviews of our approach.

Figure 1 shows the schematic diagram of our approach. In the following section, each part is described in detail.

Assumption of Surface Normal

Generally, 2D images taken of a natural scene do not include surface normal information. To apply nonphotorealistic shading to these images, we must first assume the surface normals. In SFS, surface normal vectors are computed under the following constraints: (a1) the luminance variation due to shading is useful as an indicator of the shape and (a2) the depth value is strongly related to the luminance distribution of the object. The luminance of the object also increases as the distance to the object from the observer decreases. Therefore, in SFS, the depth value $D(x,y)$ at pixel (x,y) is defined as the luminance at pixel (x,y) in the 2D image. Further, the surface normal $\boldsymbol{n}$ at pixel (x,y) is obtained by calculating the differential value of luminance.[17,18] We assume the surface normals at pixel (x,y) using this approach. In this case, the z axis is set perpendicular to the xy plane, which compiles the pixel (x,y) in the 2D image. The positive direction of z is toward the observer,

$$n(x,y) = (n_x(x,y), n_y(x,y), n_z(x,y))^T = \left(-S\frac{\partial L(x,y)}{\partial x}, -S\frac{\partial L(x,y)}{\partial y}, 1\right)^T, \tag{1}$$

where $L(x,y)$ is the luminance distribution at pixel (x,y), T is the transposition, and S is the positive coefficient used to emphasize the contrast near the contour.

As shown in Eqs. (2)–(4), the coefficient S is controlled so as to increase the value S according to the intensity of edge *Edge* at pixel (x,y),

$$Edge = \sqrt{\left(\frac{\partial L(x,y)}{\partial x}\right)^2 + \left(\frac{\partial L(x,y)}{\partial y}\right)^2}, \tag{2}$$

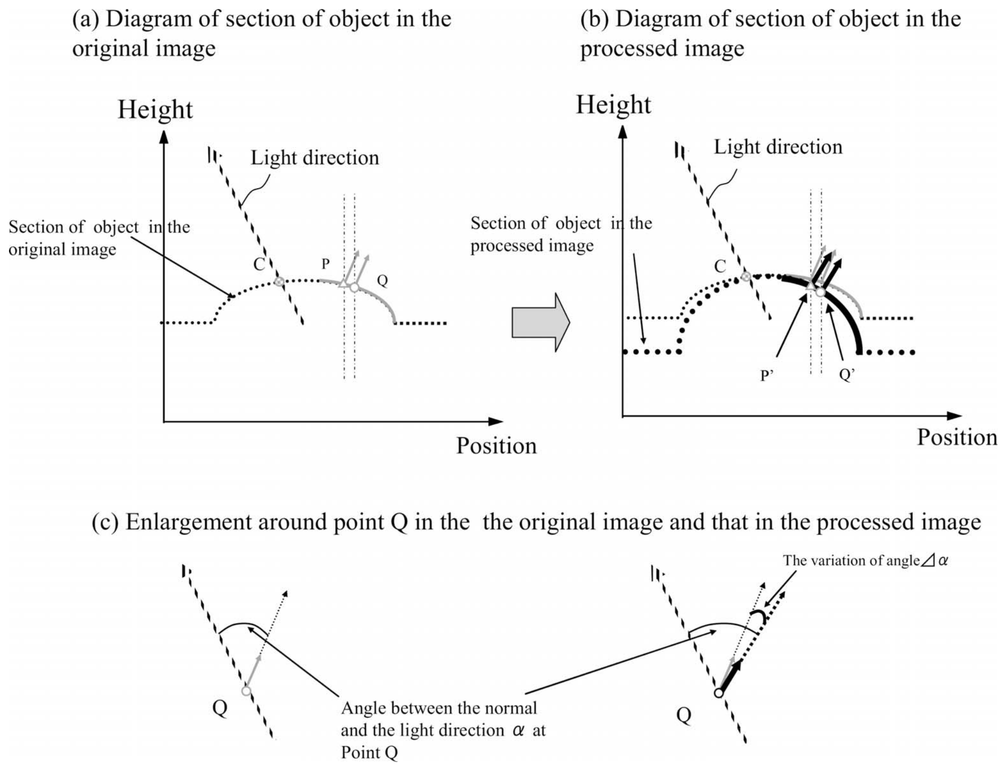

Figure 2. Diagram of modification of azimuth of normal vectors.

$$TmpS = SMax \cdot \exp\left(-\frac{(Edge - MaxEdge)^2}{SDelta^2}\right), \tag{3}$$

$$S = 1.0 + TmpS, \tag{4}$$

where $SMax$ and $SDelta$ are positive coefficients, and $MaxEdge$ is equivalent to the maximum value of the intensity of edge $Edge$ in the image. The surface normal $n(x,y)$ is calculated by Eqs. (1)–(4) to emphasize the edge component. When the intensity of edge $Edge$ is low, the coefficient S is set to 1.0, and when the intensity of edge $Edge$ is high, S is set to a large value. That is, the component $n_x(x,y)$ or $n_y(x,y)$ in surface normal $\boldsymbol{n}(x,y)$ are emphasized so that the intensity of edge $Edge$ is larger.

For enhancing the 3D shape by our approach, we are first required to determine the "*global shape information*" from the normal obtained by Eq. (1). The global shape information can in turn be represented by a gentle or smooth transition of the normal distribution. In short, the gentle transition of normals is indispensable to enhance the 3D shape with gentle gradation. As the surface normal obtained by Eq. (1) varies on a pixel-by-pixel basis according to the pixel luminance, we use a bilateral filter to smooth the components of the normals obtained by Eq. (1). The filter is tunable to spatial scales as well as luminance. Each component is filtered at the surface normal $\boldsymbol{n}$ obtained by Eq. (1). This filter is defined as follows:

$$on_s(x,y) = \frac{\sum_{u=-f}^{f}\sum_{v=-f}^{f}(B(x,y,u,v)n_s(x+u,y+v))}{\sum_{u=-f}^{f}\sum_{v=-f}^{f}(B(x,y,u,v))}, \tag{5}$$

$$B(x,y,u,v) = G_D(\sqrt{u^2+v^2},\sigma_D)G_L(|L(x+u,y+v) - L(x,y)|,\sigma_L), \tag{6}$$

$$G_K(r,\sigma_K) = \exp\left(\frac{-r^2}{\sigma_K^2}\right) \quad (K = L,D), \tag{7}$$

where n_s is the s component of the normal $\boldsymbol{n}$ obtained by Eq. (1) and on_s is the s component of the smoothed normal $\boldsymbol{n}$. The kernel B is composed of two Gaussian filter kernels G_D and G_L with kernel widths σ_D and σ_L, respectively. This filter is adapted for each component at the surface normal $\boldsymbol{n}$ obtained by Eq. (1).

Modification of the Normal Vector Azimuth

The shading approach controls the azimuth of the normals on the basis of the angle between each normal and a given light source direction. For controlling the azimuth of the normals, we assume that the enhancement of the perception of the 3D shape is strongly related to the emphasis of the curvature of the shape near the corresponding area. The curvature of the surface shape is closely related to the gradient of the luminance near the corresponding area. Therefore, by this approach, the azimuth of the normals is modi-

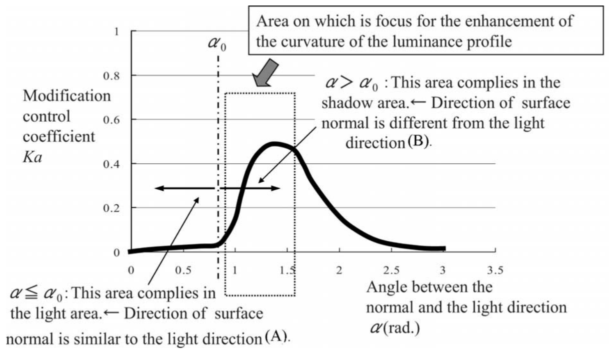

Figure 3. Variation in control coefficient with α.

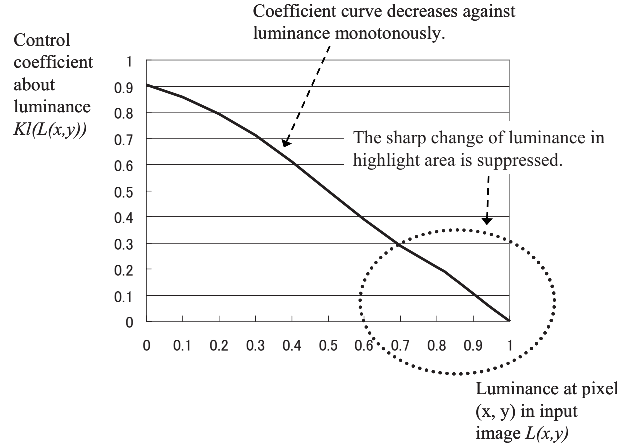

Figure 4. Variation in control coefficient with luminance at each pixel.

fied mainly to enhance the curvature of the luminance on the area with the extracted normals as shown in Figure 2.

Fig. 2 shows the section example of the object in plane composed of light direction and surface normal. Figs. 2(a)–2(c) show the section in the original image, in the processed image, and the enlargement around point Q, respectively; P and Q show the points in original image and P' and Q' show the points corresponding to P and Q in the processed image. As shown in Figs. 2(a)–2(c), the azimuth of the normal at point Q is rotated to enhance the curvature of the luminance around point Q by the shading approach. That is, the proposed approach controls the angle α at object point Q between the normal and a given light direction to enhance the curvature of the luminance around point Q.

Now, it is well known that humans by default assume that a light source is located above their head. Moreover, more recent studies have revealed that the preferred light source position is on the left side above the head rather than straight above.[20] Therefore, we assume that the light direction points toward the upper left of the image. Equation (8) shows the variation $\Delta\alpha$ in the angle α between each normal and a given light illumination direction at pixel (x,y). $Ka(\alpha)$ is the modification control coefficient function of angle α; $\Delta\alpha_c$ is the initial positive value, which implies that the shade strength is controlled by the user. $L(x,y)$ shows the luminance at pixel (x,y),

$$\Delta\alpha = Ka(\alpha)Kl(L(x,y)) \times \Delta\alpha_c. \tag{8}$$

Figure 3 shows the variation in the control coefficient function with α; α_0 is the angle between the normal at the pixel, where the luminance is locally constant and a given light direction. As shown in Fig. 3, the area in (A) incorporates the light area generated by a given light source direction and the area in (B) incorporates the shadow area generated by the same light source direction. The area enclosed by the rectangle in Fig. 3 is the area that contains the extracted normal with a gradual luminance distribution. To emphasize primarily the curvature of the luminance in the enclosed area, $Ka(\alpha)$ is controlled such that its value near the corresponding angle α between the normal and the direction of the light source increases. Further, $Ka(\alpha)$ decreases as α increases.

Second, $Kl(L(x,y))$ is the control coefficient of the input luminance. It is controlled to suppress the excess modification of angle α in the highlighted area. Figure 4 shows the variation in the control coefficient with the input luminance.

Last, a modulation component $\Delta\alpha$ of angle α is transformed into the variation in the luminance $\Delta L(x,y)$ at pixel (x,y). We assume that the diffused reflection component $L_l(x,y)$ by Lambert's reflectance model is modified mainly by our shading and the variation in luminance is computed by the following Eqs. (9) and (10):

$$\Delta L(x,y) = \frac{dL_l(x,y)}{d\alpha} \times \Delta\alpha, \tag{9}$$

$$L_l(x,y) \propto L(x,y)\cos\alpha,$$

$$L_l(x,y) = K_{\mathrm{Lam}}L(x,y)\cos\alpha, \tag{10}$$

where K_{Lam} denotes the coefficient of the diffused reflection component, and we use $K_{\mathrm{Lam}}=1.0$ as this coefficient.

Enhancement of Range of Modified Luminance

When the shading approaches are employed, there is a tendency that the luminance distribution in a modified image is compressed to some extent. Therefore, we carry out the tone mapping process to improve the reduction in the average luminance in the modified image. The luminance distribution in the modified image is transformed on the basis of the relation between the average luminance in the input image and that in the modulated image.

First, the dynamic range of the luminance in the modified image is enhanced to the range of the luminance in an input image. Next, a tone mapping process is adopted to increase the luminance distribution in a modified image.

Here, we propose that the shading addition to the shadow or highlighted area has a significant effect on the human perception of a 3D shape. Further, the use of tone mapping greatly increases the luminance distribution; tone mapping may cause the saturation of the luminance in a shadow or highlighted area, which is a drawback. Therefore, by using the tone mapping function, we primarily improve

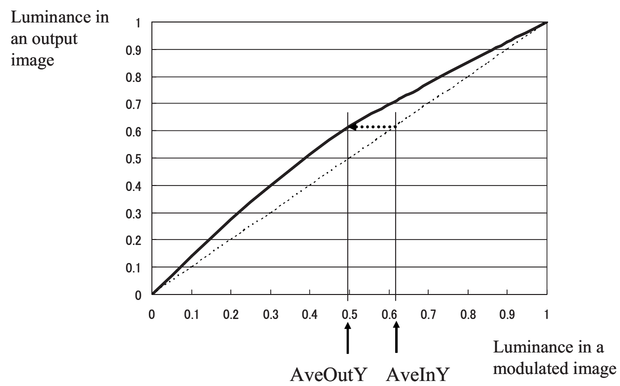

Figure 5. Tone mapping function in the enhancement of the range of modified luminance.

the luminance of that area of the image, where the luminance value is close to the center of the dynamic range.

Figure 5 shows an example of tone mapping. This figure shows the output luminance after tone mapping to the luminance modified as described above. In Fig. 5, *AveInY* is the average luminance in the input image and *AveOutY* is the average luminance in the modified image whose range is enhanced to the range of the luminance in the input image. By using tone mapping, the average luminance *AveOutY* in the modified image is transformed into the average luminance *AveInY* in the input image. This function can increase the luminance to the intermediate level of the dynamic range in the image by adding an offset value to it. On the other hand, this function suppresses the saturation of the luminance in a shadow or highlighted area. Therefore, as shown in Fig. 5, we use tone mapping to improve the reduction in the luminance distribution of a modified image. Then, we define the shading approach as the "fixed light shading approach."

VARIANT OF FIXED LIGHT SHADING APPROACH (ADVANCED SHADING APPROACH)

Above, we assumed that the light direction points toward the upper left of the image on the basis of recent researches in the field of human vision psychology.[20] However, when the luminance distribution in the input images is taken into consideration, a better light direction than the upper left light direction may exist from the viewpoint of the natural enhancement of the 3D shapes.

Then, we investigated the process by which the most suitable light direction is selected according to the luminance distribution in images. We accordingly propose the previous shading approach combined with the selection process of light direction to enhance the 3D appearance in a 2D image with more efficiency. Now, we define this variant of the fixed light shading approach as the advanced shading approach.

The outline of the process that selects the suitable light direction is shown in Figures 6 and 7. The objectives of this selection process are as follows:

(q1) A suitable light direction vector is selected from eight candidates of the light direction vector $\nu L^k = (L_x^k, L_y^k, L_z^k)$ $(k=1,2,\ldots,8)$, as shown in Fig. 6.

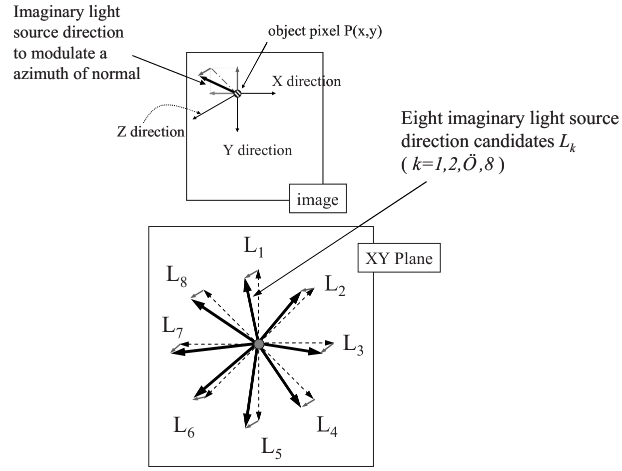

Figure 6. Definition of light direction candidates.

(q2) A suitable light direction vector is selected to enhance the natural 3D appearance with more efficiency when modulating the azimuth of the normal in an input image, as described previously.

(q3) Image distortion, which occurs due to the rapid variance of the luminance in a modified image by modulating the azimuth of the normal on the basis of the selected light direction are not generated.

On the basis of the above mentioned objectives, the selection of the suitable light direction vector is carried out as follows:

(1) First, the areas C^k $(k=1,2,\ldots,8)$ that are used to select the suitable light direction are extracted for every light direction candidate. In Fig. 3, the enclosed area is the area that contains the extracted normal with a gradual luminance distribution. Further, the normal is modulated to emphasize primarily the curvature of the luminance in these areas. Then, while calculating the suitable light direction, we extract a group of pixels contained in the above areas of an input image for each light direction. The C^k $(k=1,2,\ldots,8)$ value represents this group for the corresponding light direction νL^k. In Fig. 7, area C^k is shown as the white area corresponding to νL^k.

(2) Second, at each pixel $p_j^k(x_j^k, y_j^k)$ included in the area C^k with the light direction vector νL^k, the differential vector of luminance νIp_j^k in an input image and that of luminance νMp_j^k in a modulated image are calculated. Further, the cosine value $\cos \beta_j^k$ of the angle β_j^k between the vectors νIp_j^k and νMp_j^k is computed for each pixel p_j^k in C^k.

(3) When the cosine value $\cos \beta_j^k$ at pixel p_j^k satisfies Eq. (11), the luminance transition of an input image and that of a modulated image are aligned along the same direction. A large variance in the direction of the luminance transition may cause a distortion in the image quality. Conversely, we think that the variance causes a change in the per-

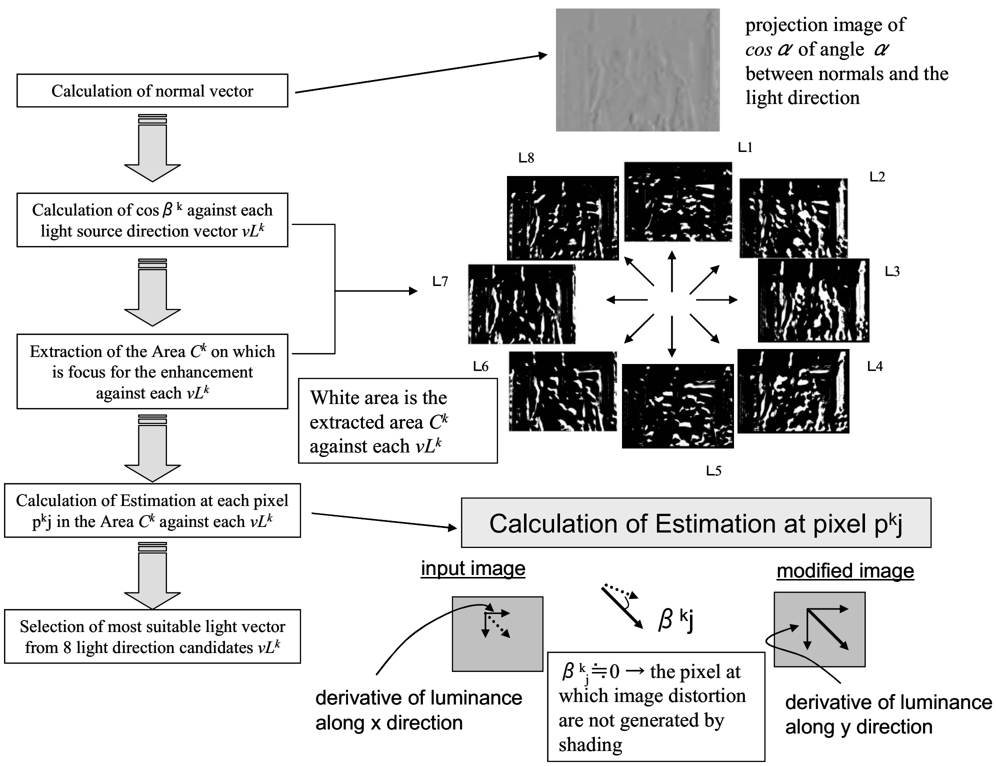

Figure 7. Selection process of suitable light source direction.

ceived texture, etc. In order to avoid this change, we should investigate whether or not the direction of the luminance transition in a modulated image is consistent with that in the input image for the pixels in area C^k. Subsequently, the number of pixels that satisfies Eq. (11) ($SumP^k$) is calculated for each light direction candidate vL^k. Here, $Th1$ has a predetermined positive value.

$$\{p_j^k | Th1 \leq \cos \beta_j^k \leq 1.0, (p_j^k \in C^k)\}, \qquad (11)$$

(4) $Eval^k$, which shows the probability of the light direction candidate k, is calculated as

$$Eval^k = \frac{SumP^k}{\sum_{k=1}^{8} SumP^k}. \qquad (12)$$

(5) The $LL(1 \leqq LL \leqq 8)$ light direction candidates with large values are selected. The revised definition of vBL^k is the light direction vector vL^k that was rearranged so that the value of $Eval^k$ became large. Using the selected light direction vector, the weighted average vector vAL is calculated as

$$vAL = \sum_{m=1}^{LL} (vBL^m \mu^m), \qquad (13)$$

$$\mu^k = \frac{Eval^k}{\sum_{m=1}^{LL} Eval^m}, \qquad (14)$$

(6) Finally, the light direction vector vL^k nearest to the weighted average vector vAL of the eight light direction candidates is concluded as the suitable direction of a light source.

EXPERIMENTAL RESULTS FOR THE FIXED LIGHT SHADING APPROACH

In this section, by experimental simulation we compare the output image obtained by fixed light shading approach, which uses a fixed upper-left direction as described above, with the input image.

Simulation Condition

We visually investigated natural 2D images (725×510 pixels and 726×1024 pixels). The kernel size of the bilateral filter in calculating of surface normal at each pixel was 41×41 pixels. The light source direction was the upper left of the image and the light source was assumed to be a parallel light source.

Estimation of Normal Vector

Figure 8 shows the angles ($\cos \alpha$) between the normal n at pixel (x, y) and the upper-left light direction for the sample image shown in Figure 9(a). Fig. 8(a) shows the case of the normal computed from the luminance gradient of the original image and Fig. 8(b) shows the case of the normal obtained by the bilateral filter. As shown in Fig. 8, $\cos \alpha$ is transformed to a pixel value in the range 0–255. The pixels in the highlighted area imply that the direction of the normals and light is almost the same. On the other hand, the pixels in the shadow area imply that the normal and light are in the opposite direction. The normal vectors in Fig. 8(b)

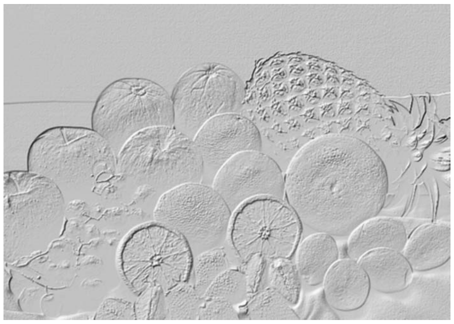

(a)

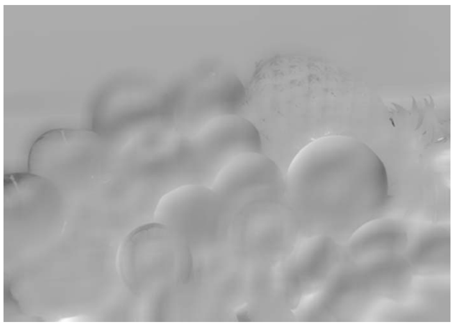

(b)

Figure 8. Projection image of cos α of angle α between the normals and the light direction. (a) Image that conveys cos α computed from the normal by the difference in luminance. (b) Image that conveys cos α computed from the normal by our approach.

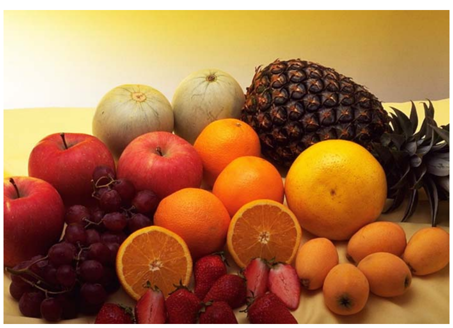

(a)

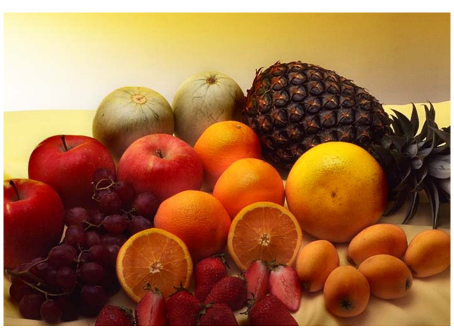

(b)

Figure 9. Comparison of the input natural image and the output image obtained by our approach. (a) 2D natural input image 1. (b) Output image 1 by our approach. Available in color as Supplemental Material on the IS&T website www.imaging.org.

(a)

(b)

Figure 10. Comparison of the input natural image and the output image obtained by our approach. (a) 2D natural input image 2. (b) Output image 2 by our approach. Available in color as Supplemental Material on the IS&T website www.imaging.org.

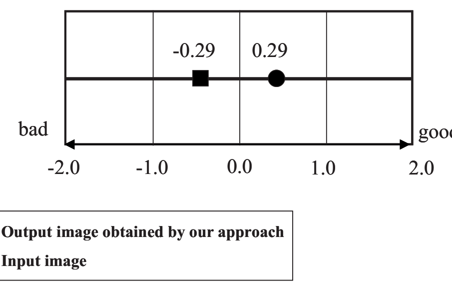

Figure 11. Evaluation of the enhancement of 3D appearance.

(a)

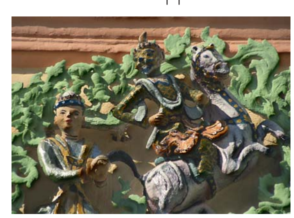

(b)

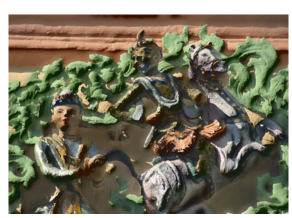

(c)

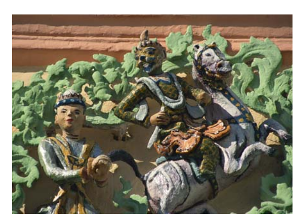

(d)

Figure 12. Variation in the output image with the enhancement strength parameter. (a) 2D natural input image 3. (b) Output image 3 for default strength. (c) Output image 3 for large strength. (d) Output image 3 for low strength. Available in color as Supplemental Material on the IS&T website www.imaging.org.

was calculated for $SMax=5.0$ and $SDelta=0.5$ in Eq. (3). As compared with Fig. 8(a), Fig. 8(b) shows resulting normals that convey coarse shape information; however, the normals near the textured area, edge, or the boundary where the pixels have comparatively significant luminance levels in the image are suppressed by the bilateral filter. That is, Fig. 8(b) implies that only the global shape information and not the local shape information are obtained by this method.

Results of Natural Images

Figures 9 and 10 show the original natural image and a sample of the output image derived from the original image, as obtained by our approach. These images were calculated for $\Delta\alpha_c=4.5$. Figs. 9(a) and 10(a) show the original images and Figs. 9(b) and 10(b) show the output images obtained by our shading approach, respectively. The output image shown in Fig. 9(b) is better than the original images from the viewpoint of perception of the 3D shape, and shading enhancement is employed for the area with gentle curvature such as the spherical surface of the fruits. On the other hand, the luminance profiles of the texture and edges remain virtually constant. As a result, there is no variation in the texture in the output image, and we confirm that the perception of the 3D shape of the objects in the output image is enhanced from the viewpoint of human vision. An enhancement of the 3D appearance is observed in both Figs. 9(b) and 10(b). In Fig. 10(b), enhancement is employed for the area such as the eye or cheek surface of the long-nosed Japanese goblin. These results suggest that our approach enhances the 3D shapes naturally without the addition artifacts on the texture or edges. Additional experimental simulations were performed using several parameters for many image samples, and we confirmed that results similar to the above were obtained. Therefore, we have shown that our approach of focusing on the global curvature of the object enables 3D appearance enhancement even in a 2D image without provided depth information.

Results of Subjective Test

We conducted a subjective test to evaluate the 3D appearance of the output images obtained by our shading approach. We used the variation in Sheffe's method of paired comparisons. Sheffe's method of paired comparison is a subjective evaluation method that simultaneously gives two image samples S_i and S_j to subjects and requests to evaluate the preference of relative 3D appearance of the two images according to Table I. In Table I, S_j shows the image presented in right area and S_i shows the one presented in left area to the each subject. In the test, subjects were simultaneously shown pairs of input and output images; the latter obtained by our approach. Each pair of images was displayed on a 50 in. plasma display. Each subject evaluated a pair of images which were presented at a viewing distance of 200 cm in the darkroom. In addition, the presentation order of the evaluation images was carried out at random, and the presentation position on the display was also determined at random. The number of evaluation images was 90. Three display experts participated in the test; all were male and in the age range from 30 to 50 years. The test was conducted twice for each subject. That is, the total number of evaluation sets is $(2 \text{ orders} \times 3 \text{ operators} \times 2 \text{ trials} \times 90 \text{ samples}) = 180$. One paired set was presented for 10 s, and a blank display period of 2 s was inserted before the presentation of the next image pair so that the result should be unaffected by the previous evaluation.

Table I. Rating category of the Sheffe's method of paired comparison.

Rating category	Score
S_j is worse than S_i	−2
S_j is a little worse than S_i	−1
S_j is almost equal to S_i	0
S_j is a little better than S_i	1
S_j is better than S_i	2

S_j represents the image which is displayed on the right from the subject.

Table II. Result of analysis of variance rid comparison.

Source of variance	S.Sq.	d.f.	M.sq.	F0
Original or output (A)	365.17	1	365.17	13.32[a,b]
Image (B)	30.0	89	0.34	0.01
Position (C)	30.0	1	30.0	1.09
Subject (D)	30.0	5	6.0	0.22
$A\times B$	32500.16	89	365.17	13.32[a,b]
$A\times C$	365.17	1	365.17	0.50
$A\times D$	69.11	5	13.82	0.01
$B\times C$	30.0	89	0.34	0.001
$B\times D$	13.94	445	0.03	0.08
$C\times D$	11.01	5	2.20	
Error	9595.44	350	27.42	
Total	43040	1080		

[a] $p<0.01$.
[b] $p<0.05$.

Figure 11 shows distance scales for the process images using Sheffe's method. The average preferences of 3D appearance of the input images and that of the output images obtained by our approach are shown on this scale. As shown in Fig. 11, it is confirmed that the output images obtained by our approach are better than the input images in terms of 3D appearance. Moreover, we investigated whether the distance between two average preferences of 3D appearance was significant, with 1% and 5% degrees of statistical risk p. Table II, which shows variances, indicates that the implementation of the shading approach affects the perception of 3D appearance. That is, our processing is a factor influencing the perception and the difference between input image and output image obtained by our approach was significant ($p<0.01$). As this result, Sheffe's method proves that our proposed approach is effective in enhancing the 3D appearance of 2D input images.

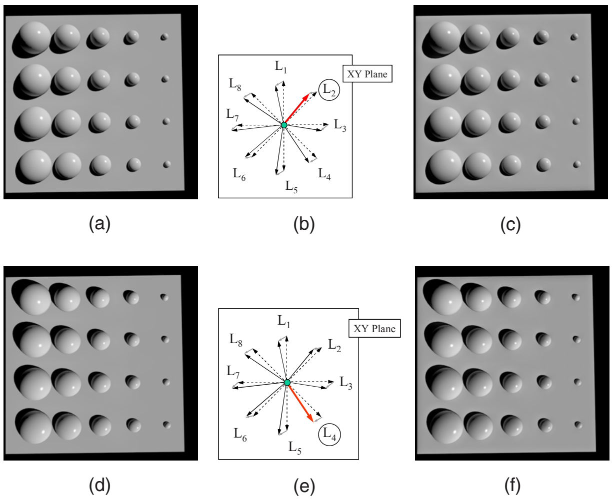

Figure 13. Example of CG images used for the evaluation of the selection of a suitable light direction. (a) CG input image with an upper-right light direction *L*2. (b) Selected light direction for (a) (upper-right: *L*2). (c) Output image for (a). (d) CG input image with a down-right light direction *L*4. (e) Selected light direction for (c) (lower-right: *L*4). (f) Output image for (c).

Variation in Shade Strength Parameter

In this section, we show the investigation of the influence on the output image quality of the variation in shade strength parameter $\Delta\alpha_c$. As shown in Eqs. (9) and (10), as the parameter $\Delta\alpha_c$ increases, the strength of enhancement increases, and the curvature of the luminance on the corresponding area increases monotonically. It is necessary to visually verify the limits of the strength parameter. Figure 12 shows the samples of output image obtained by our approach for three values of the shade strength parameter $\Delta\alpha_c$: (a) shows the input image and (b) shows the output image using the default value $\Delta\alpha_c=4.50$. Figs. 12(c) and 12(d) show the images using a large value $\Delta\alpha_c=7.5$ and small value $\Delta\alpha_c=2.25$, respectively. As shown in these figures, the enhancement of 3D shape increases with the shade parameter. On the other hand, our approach does not have the severe disadvantage of causing a tone reversal in the output image. However, the decrease in luminance in shadow areas or near boundaries increases with the shade parameter, and over enhancement is observed at some pixels near a boundary, which accordingly have a normal opposite to the given light direction, as shown in (c). From the viewpoint of image quality, we suggest that the strength parameter in (c) is nearly equal to the upper limit. The effect of enhancement decreases as the shade parameter goes to zero and, from the viewpoint of effectiveness, we think the strength parameter in (d) is nearly equal to the lower useful limit. Additional experiments have been conducted using many image samples and various parameters, and similar results have been observed.

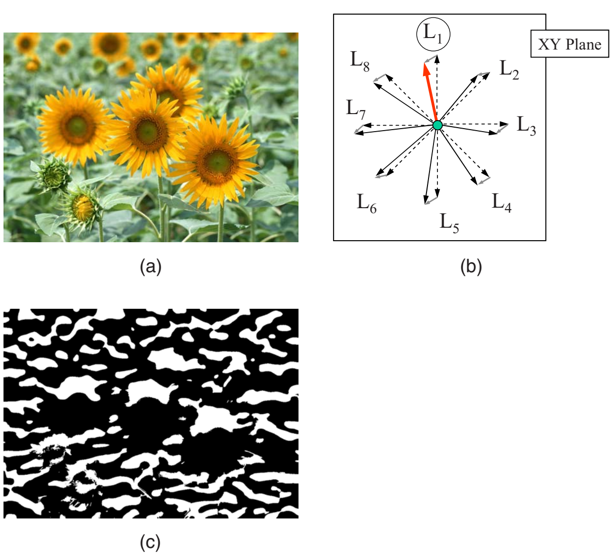

Figure 14. Example of images for which the suitable light direction was obtained by our selection approach. (a) Input image with upper light direction *L*1. (b) Selected light direction for (a) (upper: *L*1). (c) Extracted area *C*1 against light direction *L*1.

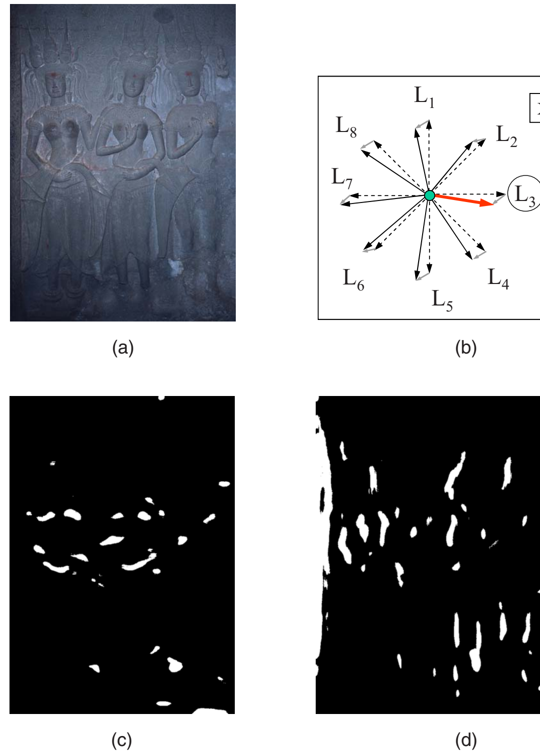

Figure 15. Example of images for which the suitable light direction is not consistent with the light direction perceived by humans. (a) Input image with upper light direction *L*1. (b) Selected light direction for (a) (right: *L*3). (c) Extracted area *C*1 against light direction *L*1. (d) Extracted area *C*3 against light direction *L*3.

EXPERIMENTAL SIMULATION RESULTS FOR ADVANCED SHADING APPROACH

In this section, by experimental simulation, we evaluate the accuracy of the selection of a suitable light direction. Then we compare the output image obtained by the advanced approach, which uses a suitable light direction described above, with the input image and the output image obtained by a fixed upper-left light source direction. We show that the advanced approach can enhance the perception of the 3D shape with more efficiency.

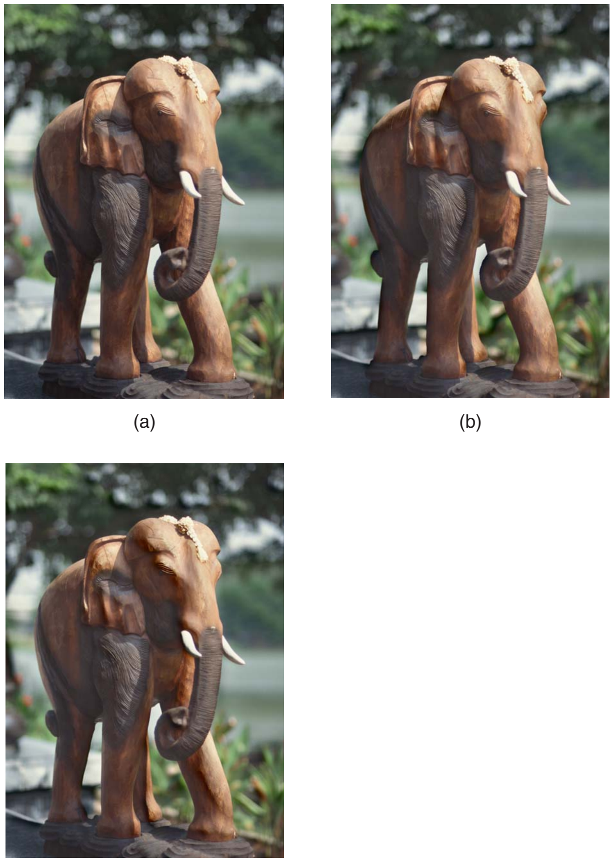

Figure 16. Comparison of output images obtained by use of a predetermined light direction (upper-left light: $L8$) and that obtained by the suitable light direction (upper-right light: $L2$). (a) 2D input image. (b) Output image obtained using the predetermined upper-left light direction. (c) Output image obtained using the more suitable upper-right light direction. Available in color as Supplemental Material on the IS&T website www.imaging.org.

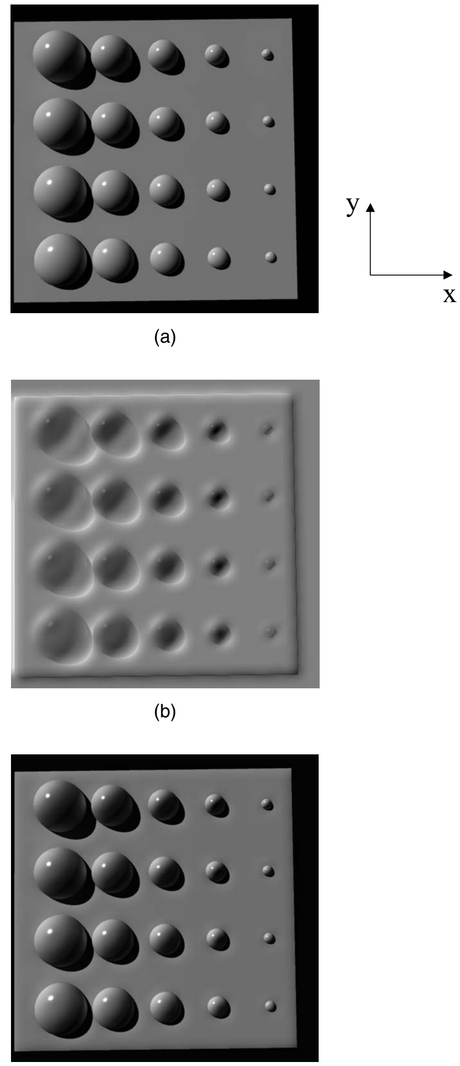

Figure 17. Comparison of the CG input image and the output image obtained by our approach. (a) 2D input image obtained by CG tool. (b) Image that convey cos α computed from the normal obtained by our approach. (c) Output image obtained by our approach.

Result of the Selection of a Suitable Light Direction

In this section, we describe the evaluation results for the accuracy of the selection of a suitable light direction using the selection approach previously described. First, by using 2D images (600×600 pixels) captured by a CG tool, e.g., SHADE 8.5,[21] we evaluated the accuracy of the selection of a suitable light direction. Figure 13 shows examples of CG input images captured by using CG hemisphere with each fixed light source direction from Fig. 6. These images are actually composed of objects with different heights and captured by a CG tool. Figs. 13(a) and 13(b) show the input images with an upward-right light direction $L2$ and with a downward-right light direction $L4$, respectively. Figs. 13(c) and 13(d) show the corresponding output images obtained by the advanced shading approach. The simulation was conducted under the same condition for calculating of the surface normal in the previous section. The selection condition was defined as $LL=3$ and $Th1=0.8$. As a result for these CG input images, we first confirmed that the corresponding light direction for each CG input image can be selected by our selection approach.

Next, we evaluated the accuracy of selection of a suitable light direction for 110 natural images. This simulation was also conducted under the same condition for calculating of previous CG input images. From the estimation simulation of 110 natural images, we could infer that the rate of selection of the light direction, consistent with the light direction perceived by human observers as the most suitable direction, was 80%.

Here, Figures 14 and 15 show examples of input natural images, the selected light direction obtained by our approach, and the extracted area C^k, against the selected light direction or a suitable light direction as shown in Fig. 7. In Figs. 14 and 15, (a) shows the input image and (b) shows the selected light direction to which the circle is added; (c) shows the extracted area C^1 against the selected light direction $L1$. In Fig. 15, (d) shows the extracted area C^3 against the suitable light direction $L3$ perceived by human. In (c) and (d), the white area is the extracted area C^k against corresponding L^k. Fig. 14 shows a sample for which the suitable light direction can be obtained by our approach, and Fig. 15

shows an example for which the selected light direction is not consistent with the light direction perceived by humans.

As shown in Fig. 14(c), we estimate that the number of the pixels in the extracted area C^1 is necessary to select this light direction as the suitable light direction. But, in Figs. 15(c) and 15(d), the number of the pixels in the extracted area C^1 is insufficient for selecting the direction $L1$ as the suitable light direction; the number of the pixels in the extracted area C^1 is less than that in the extracted area C^3 for light direction $L3$. We think that this may be caused by the large flat areas in which there is little variance in luminance. To improve the rate of selection of suitable light direction, it is necessary to investigate the autotuning of parameters for selecting light direction. Selecting suitable directions of the light sources in the image by using the luminance distribution is important to shading in the field of CG. However, it is generally difficult to achieve this direction for natural images. We therefore do not contend that an accurate orientation of light sources in the image can by determined by this selection approach. However, as viewpoint of the high rate of selecting a suitable light direction previously demonstrated, we think that our selection approach is adequate to enhance the 3D appearance of a 2D image.

Result of the Advanced Shading Approach

Figure 16 shows the input and output images employing a predetermined upper-left light direction and the output image is obtained by employing a suitably selected light direction. Here, the two output images are obtained under the same conditions employed above. And the previous values were applied as the selection condition, e.g., $LL=3$ and $Th1=0.8$. The number of pixels in the input image along the x and y directions are 726 and 1024, respectively.

As shown in the input image, the light source direction appears to be the upper-right direction rather than the upper-left direction. In the case of the output image obtained by using the upper-left light direction, there is no discontinuity in the output image. However, the enhancement in the 3D appearance is inhibited. For example, these trends can be seen in the left forelimb or in the back of the wooden elephant. On the other hand, there is no discontinuity in the output image obtained when an upper-right light direction is selected. Moreover, the 3D appearance effect is further enhanced at the left forelimb or at the back of the figure. Further, the unevenness in the face of the figure is enhanced. Thus, the 3D appearance effect can be further enhanced by implementing the process for determining a suitable light direction on the basis of the luminance distribution in an image.

DISCUSSION

On the basis of the previous test for natural images, we cannot investigate the enhancement of the 3D shape by our approach quantitatively. Therefore, to demonstrate the enhancement of the 3D shape by our approach quantitatively, we use the original CG image that is actually arranged by objects with different heights. Further, we investigate the enhanced shape surface of the output image of this CG image. Next, we discuss the possibilities of advanced shading approach on the view of effect using multiple light source directions.

Quantitative Evaluation Using CG Images

As described above, we visually tested the 2D images (600×600 pixels) captured by a CG tool.[21] Moreover, we used a CG hemisphere with a light source fixed on the upper-left side of the image. The estimation conditions are the same as previously employed. Figures 17(a)–17(c) show the original synthetic image (a), angles ($\cos\alpha$) between the normal $\boldsymbol{n}$ at pixel (x,y) and the upper-left light direction (b), and output image obtained by our approach (c). Specifically, Fig. 17(c) was calculated for $\Delta\alpha_c=3.0$. The CG original image shown in Fig. 17(a) is obtained by arranging four convex half-spheres and the height of the hemispheres increases from the bottom along the y-direction in a CG image. Fig. 17(b) shows the normals that convey the coarse shape information. Further, as compared to the image in Fig. 17(a), the output image shown in Fig. 17(c) is better from the viewpoint of the perception of the 3D shape.

As mentioned above, the CG image is composed of convex half-spheres whose height becomes greater as it moves upward from the bottom along the y-direction. This process controls the curvature of luminance near an object pixel according to the angle between the normal in the object pixel and a given light direction, and in the case that the luminance distribution of the object in the output image is similar to that of the hemisphere, which is taller than the object in input image, the object in output image may have the 3D appearance similar to this latter hemisphere in the input image. Therefore, we compare the luminance distribution of the object in the output image with that of the hemisphere, which is taller than the object in the input image. Accordingly, we evaluated the degree of enhancement of the 3D characteristic quantitatively by checking whether the luminance distribution of a given object in the output image is similar to that in the input image.

Figure 18 shows the variation in luminance along the line RQ of objects A and B shown in Fig. 18(a). The thin black and bold blue lines show the variation in the luminance of the original image along the line RQ of objects A and B, respectively. Moreover, the red line shows the variation in the luminance of the output image obtained by our approach along the line RQ of object A. In Fig. 18, both (c) and (d) are images for object A and (e) is for object B. In the original CG image, object B is set taller than object A. In (b), the bold red line is similar to the dashed blue line and not the solid line. In Fig. 18(b), object A in the output image has a profile more similar to that of object B in the original image rather than to object A in the original image. From this result, we confirm that the surface of object A in the output image expands to the same extent as that of object B in the original image. This confirms that the surface of object A in the output image is enhanced and has almost the same 3D appearance as object B.

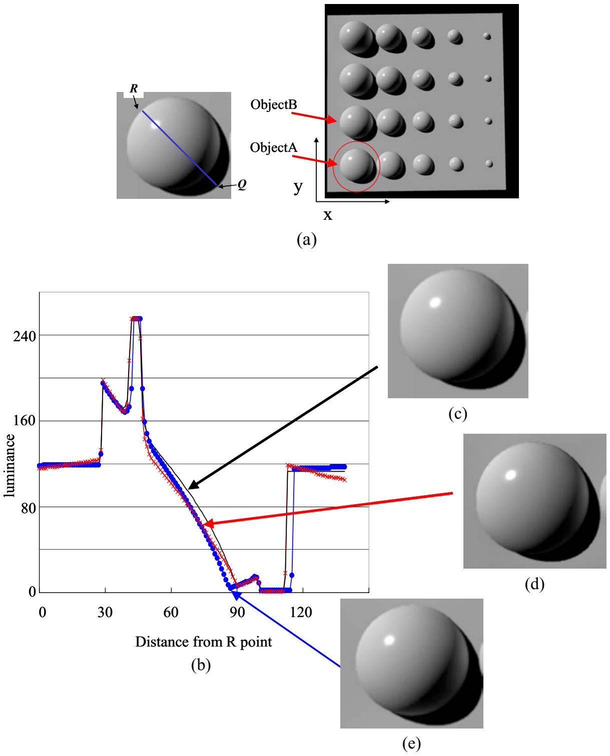

Figure 18. Hemispheres and luminance profiles along RQ. (a) Position of objects *A* and *B*, and the definition of line RQ. (b) Luminance profiles along RQ. (c) Object *A* in original image. (d) Object *A* in output Image. (e) Object *B* in original image.

Effect by Using Multiple Light Directions

In the previous section, we compared the output image obtained by the advanced shading approach, which finds a suitable light direction, and with the input image and the output image obtained by a fixed upper-left light source direction. Thus, we showed that the 3D appearance effect can be further enhanced by implementing the process for determining a suitable light direction on the basis of the luminance distribution in an image as shown in the Variant of Fixed Light Shading Approach (Advanced Shading Approach) section. However, there are few situations, which have only one light source, and, in many cases, processing using two or more light sources may be used to increase the effect given by a single light source. Then, we generated the output image by adding another light source to the first suitable light direction selected by our approach.

Next, we compared that image with the input image or that obtained by one suitable light direction. Now, when another light direction is added to the first suitable light direction, the strength parameter was adjusted so that the degree of 3D appearance by using two light directions might become comparable to that obtained using one suitable light direction. Figure 19 shows an example of the input image, the output image using one suitable light direction, and that using two suitable light directions: (a) and (b) show the input image and the output image using one suitable light direction obtained by our approach and (c) shows the output image by using the first suitable light direction and a second light direction, which is perpendicular to the selected

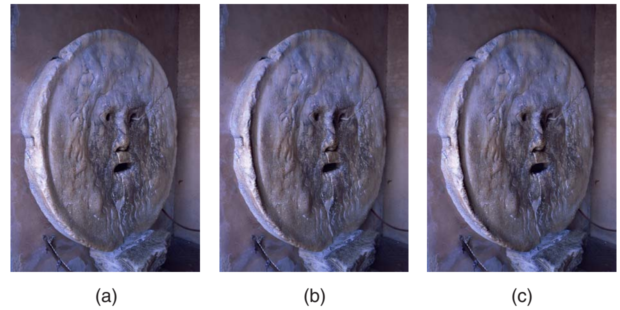

Figure 19. Comparison of the input image, the output image obtained using a suitable light direction and that obtained using two suitable light directions. (a) Input image. (b) Output image using one suitable light direction (left light: *L7*). (c) Output image using two suitable light directions (left light: *L7* and down light: *L5*). Available in color as Supplemental Material on the IS&T website www.imaging.org.

light direction. The 3D effect in the output images (b) and (c) is improved compared to the input image (a). Furthermore, as shown in (c), shade emphasis near an area, which was difficult to add using only the one light source (the areas near the upper or upper-right boundaries in the facial structure), is improved, and the 3D effect is further increased using the two suitable light directions.

From the above result, we think that a more natural improvement of 3D appearance can be obtained by using two or more light directions compared with the case of using only one suitable light direction. However, when using two or more light sources, it is necessary to select and add the other light directions, which increases the 3D effect using one suitable light direction, to the first suitable light direction obtained by our selection approach.

Application of the Advanced Shading Approach to a Movie

When our approach is to be applied to a motion picture, it is usually implemented individually for the image in each frame. In this case, a variation in the light direction selection may occur from frame-to-frame, owing to the luminance variance caused by environmental changes at the time of photography, even though the scene change is small. As a result, there is a danger of generating artifacts such as a flickering phenomenon in the movie after processing. Accordingly in the case where the proposed approach is applied to a movie, the distribution of the normal vector in an input image of a given frame is compared with that in the input image of the previous frame, and the light direction is selected appropriately.

For each pixel $p_i(x,y)$, the cosine $\cos \gamma_i^t$ of the angle γ_i^t between the normal vector presenting a given frame at time t and the that at the previous frame $(t-1)$ is calculated. The number $MSumF^t{+}{+}$ of the pixels for which $\cos \gamma_i^t$ is greater than the predetermined positive threshold $Th2$ is calculated. Further, we determine the ratio $MEval^t$ as shown in the equation below,

$$MEval^t = \frac{MSumF^t}{Total\ \ Number}. \tag{15}$$

In Eq. (15), *Total Number* shows the total number of the pixels in an image and the ratio $MEval^t$ shows the ratio of $MSumF^t$ to the total number of the pixels in an image. By comparing $MEval^t$ with a predetermined positive threshold $Th3$, we determine whether there is any major scene change as a consequence of modulating the azimuth of the normal vector. When the ratio $MEval^t$ is smaller than a predetermined threshold, the light direction is not selected for the present frame; instead, the light direction vector selected for the previous frame is employed. Moreover, in the selection of the most suitable light direction, the light vector is synthesized starting with the light direction vector in the previous time frame. We apply this synthesis process in order to decelerate the rapid change in the light direction and to suppress the flickering phenomenon in output images.

CONCLUSIONS AND FUTURE WORKS

We have proposed a nonphotorealistic shading approach for the enhancement of the surface shape in 2D images that do not have depth information (fixed light direction shading approach). This approach consists of three processes:

(p1) assumption of the surface normal;

(p2) shading approach by controlling the azimuth of the normal on the basis of the angle between the normal and a given light source direction; and

(p3) enhancement of the range of the modified luminance distribution.

Moreover, we have proposed the selection of a suitable light source direction to enhance the perception of the 3D shape more effectively and also have proposed the advanced shading approach, which incorporates a combination of the fixed light direction shading approach and the heuristic selection process of a suitable light source direction. First, we have demonstrated the performance of our approach by experimental simulation of natural images and subjective tests for the fixed light direction shading approach. Second, we have investigated the performance of our approach to the selection of a suitable light source direction and also have demonstrated that the 3D appearance can be further enhanced by the advanced shading approach. Last, we have discussed the performance of our approach by the quantitative evaluation of the CG input image and also have made visual comparison between the effects of using two light source directions and that of using one suitable light direction only.

In the course of this work, we only investigated the enhancement of 3D shapes for half-spheres; but, it is also necessary to investigate the effectiveness of the proposed approach for other objects. Therefore, in the future, we will investigate the enhancement of perception of a 3D shape for the objects such as pyramids or cubes, and, to improve the rate of selection of the most suitable light direction, we are required to investigate the influence of the parameters in selection process.

Moreover, we have investigated the possibility of using multiple light source directions from the point of view of improvement of the perception of 3D shape. However, we need to investigate the influence of multiple light source directions more quantitatively, and we also need to investigate the selection of these multiple light directions, whereby the 3D effect can be further increased. Finally, because the determination of surface normal by a bilateral filter is time-intensive, we will investigate a potential processes for the determining the surface normal more rapidly. Nevertheless, our approach enables the addition of newer attractive features to displays, which differ from the features of conventional image processing for obtaining high quality.

REFERENCES

[1] J. M. Dicarlo and B. A. Wandell, "Rendering high dynamic range images", Proc. SPIE **3965**, 392–401 (2000).

[2] E. Reinhard, M. Stark, and J. Ferwerda, "Photographic tone reproduction for digital images", ACM Trans. Graphics **21**, 267–276 (2002).

[3] P. Ledda, A. Chalmers, T. Trosciako, and H. Seetzen, "Evaluation of tone mapping operators using a high dynamic range display", ACM Trans. Graphics **24**, 640–648 (2005).

[4] E. Reinhard and K. Devlin, "Dynamic range reduction inspired by photoreceptor physiology", IEEE Trans. Vis. Comput. Graph. **11**, 13–24 (2005).

[5] J. Starck, F. Murtagh, E. Candes, and D. Donoho, "Gray and color image contrast enhancement by the curvelet transform", IEEE Trans. Image Process. **12**, 706–717 (2003).

[6] S. N. Pattanaik, J. A. Ferwerda, M. D. Fairchild, and D. P. Greenberg, "A multiscale model of adaptation and spatial vision for realistic image display", *Proc. SIGGRAPH* (ACM, Orlando, FL, 1998), pp. 287–298.

[7] T. Saito and T. Takahashi, "Comprehensive rendering of 3-d shapes", Comput. Graphics **24**, 197–206 (1990).

[8] G. Winkenbach and D. Salesin, "Computer-generated pen-and-ink illustration", *Proc. ACM SIGGRAPH 94* (ACM, Orlando, FL, 1994), pp. 91–100.

[9] A. Gooth, B. Gooth, P. Shirley, and E. Cohen, "A non-photorealistic lighting model for automatic technical illustration", *Proc. SIGGRAPH 98*, (ACM, Orlando, FL, 1998), pp. 447–452.

[10] P. P. Sloan, W. Martin, A. Gooch, and B. Gooch, "The lit sphere: A model for capturing npr shading from art", *GI 2001* (Morgan Kaufmann, Ontario, 2001), pp. 143–150.

[11] P. Cignoni, R. Scopigno, and M. Tarini, "A simple normal enhancement technique for interactive non-photorealistic rendering", Comput. Graphics **29**, 125–133 (2005).

[12] S. Rusinkiewicz, M. Burns, and D. DeCarlo, "Exaggerated shading for depicting shape and detail", ACM Trans. Graphics **25**, 1199–1205 (2006).

[13] T. Luft, C. Colditz, and O. Desussen, "Imaging enhancement of unsharp masking the depth buffer", ACM Trans. Graphics **25**, 1206–1213 (2006).

[14] D. Pearson and J. Robinson, "Visual communication at very low data rates", Proc. IEEE **73**, 795–812 (1985).

[15] A. Ni, K. Jeong, S. Lee, and L. Markosian, "Multiscale line drawing from 3D meshes", *Proc. 2006 Symposium on Interactive 3D Graphics and Games* (ACM, California, 2006), pp. 133–137.

[16] T. Judd, F. Durand, and E. H. Adelson, "Apparent ridges for line drawing", ACM Trans. Graphics **26**, 755–762 (2007).

[17] B. K. P. Horn, "Height and gradient from shading", Int. J. Comput. Vis. **5**, 37–75 (1989).

[18] A. Pentland, "Shape information from shading: a theory about human perception", *Proc. Int'l Conf. Computer Vision* (IEEE, 1988), pp. 404–413.

[19] T. Watanabe and S. Ojima, "Enhancement of 3D shape in 2D natural images using a non-photorealistic shading approach", *Proc. 2008 International Conference on Consumer Electronics: Digest of Technical Papers* (IEEE, Las Vegas, 2008), pp. 443–444.

[20] P. Mamassin, "Neural correlates of shape form shading", J. Vision **14**, 971–975 (2003).

[21] C. Satow and Y. Yonetani, *Shade design factory* (BNN, Inc., 2005).